ELSEVIER

Chemical Engineering Science 60 (2005) 3061–3079

Chemical Engineering Science

www.elsevier.com/locate/ces

Dynamic optimization of a semi-batch reactor for polyurethane production

Victor M. Zavala[a], Antonio Flores-Tlacuahuac[a,*,1], Eduardo Vivaldo-Lima[b]

[a]*Department of Chemical Engineering, Carnegie-Mellon University, 5000 Forbes Avenue, Pittsburgh, PA 15213, USA*
[b]*Departamento de Ingeniería Química, Facultad de Química, Universidad Nacional Autónoma de México (UNAM), Conjunto E, Cd. Universitaria, México, DF 04510, México*

Received 2 September 2004; received in revised form 21 December 2004; accepted 31 January 2005

Abstract

In this work, the dynamic optimization of a polyurethane copolymerization reactor is addressed. A kinetic–probabilistic model is used to describe the nonlinear step-growth polymerization of a mixture of low- and high-molecular-weight diols, and a low-molecular-weight diisocyanate. The dynamic optimization formulation gives rise to a highly complex and nonlinear differential–algebraic equation (DAE) system. The DAE optimization problem is solved using a simultaneous approach (SDO) wherein the differential and algebraic variables are fully discretized leading to a large-scale nonlinear programming (NLP) problem. The main reactor operation process control objective is the maximization of the molecular weight distribution (MWD) under a desired batch time, subject to a large set of operational constraints, while simultaneously avoiding the formation of polymer network (gel molecule). Typically, polyurethane formation is carried out using batch reactors. However, batch operation leads to attain relatively low MWD values and, if the process is not efficiently operated, there is always the possibility of obtaining a polymer network. In this work, it was found that process operation is greatly enhanced by the semi-batch addition of 1,4-butanediol and diamine, and the manipulation of the reactor temperature profile, allowing to obtain high molecular weights while avoiding the onset of the gelation point.

Keywords: Polyurethane; Semi-batch; Dynamic optimization; Simultaneous approach

1. Introduction

Batch and semi-batch reactors are widely used in the production of fine chemicals, specialities and other high value products. This type of reactors are industrially important, and particularly well-suited, for the production of polymers of varying grades whose quality is assessed in terms of strength, stiffness, processability, etc. These abstract polymer end qualities can be reduced to readily quantifiable measurements (molecular weight distribution (MWD), copolymer composition) (Tsoukas et al., 1982).

The operation of batch and semi-batch reactors is typically carried out using recipes which are based mainly on heuristics and plant experience. One of the reasons for the limited industrial acceptance of systematic procedures, such as numerical optimization techniques, for the determination of operation decisions is the need of detailed dynamic models, which might not be reliable under the degrees of sophistication required (Abel et al., 2000). Model development and validation tends to be expensive and the related uncertainty might still be high. Moreover, the present status of nonlinear optimization techniques can make sometimes difficult to solve the underlying large-scale optimization program (Boyd and Vandenberghe, 2004). Nevertheless, state-of-the-art real-time optimization, estimation and control tools have been and are under development as efficient alternative solutions, gaining industrial acceptance during the last years (Biegler and Grossman, 2004).

* Corresponding author. Tel./fax: +52(55) 5950 4074.
E-mail address: antonio.flores@uia.mx (A. Flores-Tlacuahuac)
URL: http://200.13.98.241/~antonio (A. Flores-Tlacuahuac).
[1] On leave from Universidad Iberoamericana (México City).

0009-2509/$ - see front matter © 2005 Elsevier Ltd. All rights reserved.
doi:10.1016/j.ces.2005.01.020

Using an optimization approach, operation decisions are easily subject to technical and other constraints regarding quality and safety. An operating strategy that satisfies all the process constraints and lead to optimal production normally requires the solution of highly complex optimization problems (Palanki and Vemuri, 2003). Temperature, monomer and initiator feed rates profiles are some of the most common operational policies commonly found in the optimization of discontinuous polymerization reactors. Hence, optimal operation policies might be obtained by means of a dynamic optimization framework formulation of the process control objectives. For instance, the control objective might be posed as to minimize the deviation from a desired performance criteria (such as polymer quality or costs) at the end of a proposed batch time, or alternatively, minimize the batch time obtaining the desired polymer properties subject to operational and safety constraints.

The determination of optimal operation policies by means of dynamic optimization techniques is of a major importance for actual process operation (Cuthrell and Biegler, 1989). Moreover, the complexity of such problem is related to the presence of large sets of highly nonlinear differential and algebraic equations (DAEs). There are essentially two approaches for solving DAE optimization problems (Biegler et al., 2002). In the first, or sequential approach, the optimization is performed in the space of the independent variables only by separating dynamic and algebraic equations in subproblems. These methods offer the advantage that any intermediate solution is acceptable, in the sense that it is at least feasible. However, they run into problems if the optimization algorithm requires gradient information, because standard DAEs solvers are not usually written to provide parametric sensitivities of the solution or, if provided, they might not be accurate enough for highly nonlinear models. In the second approach, the DAE optimization problem is solved by full discretization of the differential and algebraic variables, usually leading to a large-scale nonlinear programming problem. The main advantage of this method is that equality and inequality constraints are handled in a straightforward manner. The main disadvantage commonly attributed to this approach is that the number of decision and algebraic constraints tends to increase dramatically with the size of the underlying DAE system. However, state-of-the-art large-scale nonlinear programming solvers are currently able to handle 10^5–10^6 variables and constraints (Waechter, 2002; Gill et al., 1998). Hard nonlinearities (i.e., multiple steady-states, open-loop unstable points, oscillatory behavior, etc) embedded in the model are another major source of potential numerical optimization problems. Hence, solving efficiently general nonlinear large-scale optimization problems remain as a major research challenge.

Computer automation has been successfully applied to the polymerization industry for more than 25 years. Polymerization reactor control has been the focus of several research groups, and significant progress has been achieved in this area. Several reviews on the topic are available (Garcia-Rubio et al., 1982; MacGregor et al., 1984; Elicabe and Meira, 1988; Ray, 1989; Chien and Penlidis, 1990; Schuler and Schmidt, 1992; Schork et al., 1993; Dimitratos et al., 1994; Penlidis, 1994; Schork, 1994; Kiparissides, 1996; Congalidis and Richards, 1998; Kammona et al., 1999). The main aspects addressed by these research groups, as reviewed by Congalidis and Richards (1998), have been the following: (a) bulk, solution and emulsion free radical polymerization systems, (b) development and evaluation of sensors for on-line measurement and estimation of monomer conversion and polymer properties, (c) several reactor configurations used in the experimental and simulation studies, including continuous, batch, and semi-batch reactors, as well as reactor trains, (d) homopolymerization of methyl methacrylate (MMA) and copolymerizations of MMA with other acrylates, or vinyl acetate, and (e) industrial applications generally limited to polyethylene and -olefin polymerization plants. Important research studies in polymerization reactor control span a wide array of topics (Congalidis and Richards, 1998): temperature control; optimization of initiator or monomer additions; reactor temperature needed to achieve desired polymer properties in minimum time, maximize productivity in a batch or semi-batch reactor, or control de polymer molecular weight distribution; on-line state estimators of polymer properties by using calorimetric (Schuler and Schmidt, 1992), densitometry, refractometry (Kammona et al., 1999; Vega, 1997; Bahr and Pinto, 1991; Zaldivar et al., 1997), near-infrared spectroscopy (NIRS) (Dimitratos et al., 1994; Penlidis, 1994; Schork, 1994; Kiparissides, 1996; Congalidis and Richards, 1998), viscometry (Catalgil-Giz et al., 2001; Vega et al., 2001), and size exclusion chromatography (SEC) (Kammona et al., 1999), kinetic models, or neural network techniques; evaluation of advanced feedback controllers, including adaptive controllers, model predictive controllers, and nonlinear controllers; and evaluation of statistical techniques based on multiway principal component analysis for polymer reactor monitoring and control.

As observed from the short review offered above, the area of control of polymerization reactors has shown significant improvements over the years. The area of optimization of polymerization reactors, and particularly optimization of step growth polymerization reactors, had remained behind in progress. However, with the advent of new analytical techniques for measurement of polymer quality and the development of novel nonlinear optimization solution strategies (Cuthrell and Biegler, 1987), and more efficient nonlinear optimization solvers (Waechter, 2002; Gill et al., 1998), dynamic optimization has established itself as a valuable tool for tackling complex design and operation problems. In addition, the scope of dynamic optimization is extending to the execution of real-time applications for on-line purposes, including system identification and data reconciliation, model predictive control and real-time optimization (Jockenhaevel et al., 2003).

Several researchers have applied dynamic optimization techniques or optimal control theory to free-radical polymerization reactors, for the determination of optimal reactor temperature and initiator feed addition policies that minimize reaction time, and produce a polymer with desired final properties. Hicks et al. (1969) applied the maximum principle (Pontryagin et al., 1962) to a free-radical polymerization reactor, to minimize deviations of conversion, number-average molecular weight and polydispersity from their desired target values. This early attempt to solve a polymerization batch reactor optimal control problem was unsuccessful due to severe computational problems. Clough et al. (1978) applied the maximum principle to solve the minimum time problem for a batch styrene polymerization reactor. They were able to find an optimal reactor temperature profile which conformed to industrial practice. Thomas and Kiparissides (1984) applied Pontryagin's minimum principle to a batch polymerization reactor for poly-methylmethacrylate (PMMA) manufacture to calculate near-optimal reactor temperature and initiator addition policies to produce a polymer with desired conversion, number and weight average molecular weight values. Chang and Lai (1992) developed a modified two-step method to simplify the calculation procedure for estimating the optimal reactor temperature profile for MWD control. With this method, profiles of instantaneous average chain length and polydispersity, which provide a desired MWD, are estimated. Next, the time profile of the reactor temperature is obtained via tracking of the profile of instantaneous average chain length only.

Some authors (Tsoukas et al., 1982; Butala et al., 1988) have extended these techniques to the solution of multiobjective dynamic optimization problems applied to semi-batch free-radical copolymerization reactors. Tsoukas et al. (1982) results demonstrated that high compromises exist among different optimization objectives, that yield nearly utopian solutions reflecting the importance of a high level of understanding of the trade-offs between control objectives. In a more recent work (Abel et al., 2000), the productivity optimization of an industrial semi-batch reactor was accomplished under safety constraints related to reactor pressure limits. A reduced dynamic model was developed for optimization of trajectories of operation variables such as feed flowrate and temperature. Their results show that significant reductions of batch time are possible and that their extent depend on the formulation of the safety constraints.

Polyurethanes have been in the market for over 60 years. Their uses and applications are quite diverse. Created initially to rival polyamide (nylon) fibers, they are now important in fields such as flexible and rigid foams, elastomers, coatings, and adhesives, as well as in medical applications. There are several variations of polyurethanes manufacturing. Although polyurethane production is usually carried out in reaction injection molding (RIM) processes, due to the fast reaction rate of some monomers, some technologies for production of polyurethane-based adhesives use batch stirred tank reactors, where the monomers are dissolved in a solvent. Reaction conditions (mixing effectiveness, temperature, viscosity and stoichiometric ratio) play an important role in determining the final properties of the product. A highly nonlinear complex dynamic mathematical model able to describe the polyurethane copolymerization reaction system (i.e., cross-linking reactions), previously studied and experimentally validated by Vivaldo-Lima et al. (2004), is employed in this work. Hard nonlinearities were found in this model and have been reported elsewhere (Flores-Tlacuahuac et al., 2004b).

Industrially, polyurethane manufacture is normally carried out in batch reactors (Barksby et al., 2000). However, operational difficulties (i.e., the formation of a polymer network) and relatively low polyurethane MWD values, may make desired end polymer properties hard to achieve. Nogueira et al. presented an experimental study to control conversion and weight average molecular weight of polyurethane in solution step growth polymerization, using near-infrared spectroscopy (NIRS) and torquemetry (Nogueira et al., 2003). In this work, the possibility of enhancing reactor performance employing a semi-batch-like operation mode is addressed. Therefore, optimal reactants feed addition and reactor temperature profile policies for a polyurethane copolymerization semi-batch reactor are obtained by posing the problem in a dynamic optimization framework. The dynamic optimization control objective is to provide optimal operating policies (reactor temperature, monomer, diol and diamine feed rates) in order to maximize copolymer average molecular weight, while avoiding the formation of a polymer network. This undesired phenomenon might be avoided by selecting adequate optimal operation policies, forcing the gel formation avoidance as a hard constraint. The polymerization reactor behavior is governed by a set of highly nonlinear ordinary differential and algebraic equations. Simultaneous dynamic optimization (SDO), using orthogonal collocation on finite elements for temporal discretization is used, for solving the underlying DAE optimization problem. As far as we know, there are not published works related to the dynamic optimization of polyurethane batch or semi-batch reactors.

2. Process mathematical model

In this section, the mathematical model of a nonlinear step-growth copolymerization of a mixture of low- and high-molecular weight diols, and a low-molecular-weight diisocyanate, using a kinetic approach is described (Vivaldo-Lima et al., 2004). The set of polymerization reactions is carried out in a jacketed semi-batch reactor, as shown in Fig. 1. Perfect mixing as well as constant physical properties (heat-transfer coefficient, polymer mixture and monomer densities, heat capacities, etc.) have been assumed.

The kinetic model allows for the calculation of the concentrations of all species. Different reactivities for isocyanate functional groups, located in different positions of the monomer and polymer molecules, as well as the

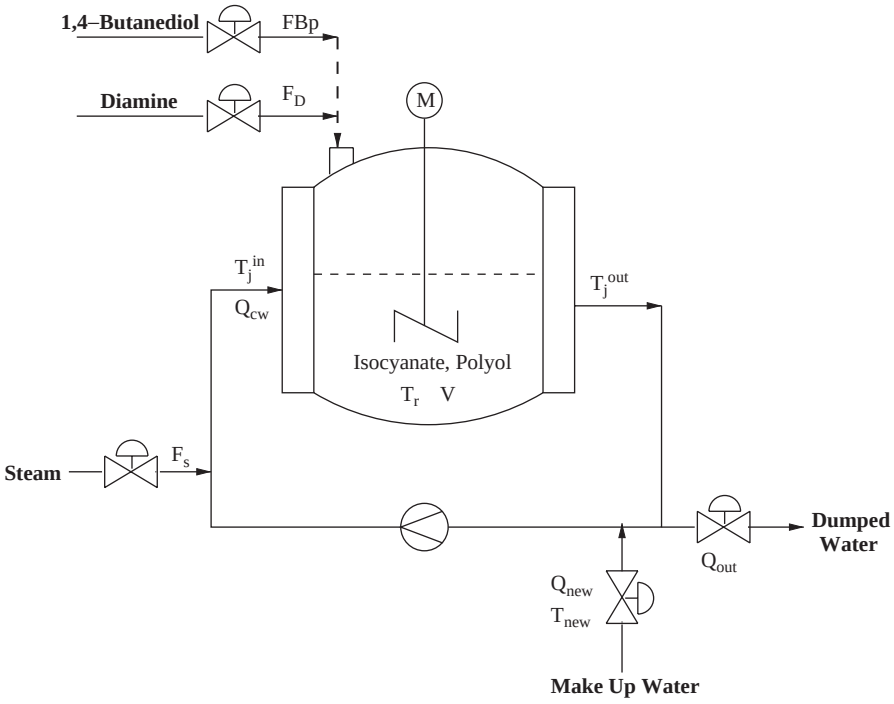

Fig. 1. Scheme of the semi-batch polymerization reactor.

hydroxyl functional groups of different molecules, are allowed. The model, developed by Vivaldo-Lima et al. (2004), uses the Macosko–Miller recursive probabilistic approach to calculate the weight average molecular weight and the gelation point. Allophanate and biuret ramification reactions are considered by the model. The model was validated experimentally for the batch reaction of methyl diisocyanate (MDI) with a mixture of a long polyol (polypropylene oxide capped with ethylene oxide) and 1,4-butanediol. Refer to (Vivaldo-Lima et al., 2004) for a complete review on the modelling and experimental validation of the copolymerization system.

It is well known that the Macosko–Miller model for calculation of weigh average molecular weight (M_w) in step-growth polymerization is only adequate for batch stirred tank reactors, and inappropriate to model continuous operation of stirred tank reactors (Dotson et al., 1996). Although the validity of the molecular weight distribution density function behind the Macosko–Miller method has not been studied for the case of semi-batch operation, it is likely that the precision of the weight average M_w calculations will be higher for semi-batch than for pure continuous operation, and if the overall amount of material fed by the inlet flow is small, compared to the mass holdup of the system. In other words, the more continuous-like the operation is, the more incorrect the predicted values of M_w will be, whereas the more batch-like the operation is, the predictions of M_w will be more accurate. The batch analysis discussed in Section 4.1 is included with the double purpose of testing the improvement on molecular weight development obtained with semi-batch addition policies and, at the same time, to make sure that the performance of the reactor is close enough to the batch operation, thus ensuring that making use of the Macosko–Miller approach for calculation of M_w is still adequate.

Heating and cooling of the semi-batch reactor is allowed by the incorporation of a heating–cooling loop system, presented in Fig. 1. Here, the cooling mode is allowed by dumping the "hot" jacket outlet cooling water Q_{out} and replacing it by the same amount of new "cold" cooling water Q_{new}. The heating mode is allowed by the direct feeding of low-pressure steam approximately at 100 °C and closing the cooling water valve. Although a common industrial practice is the indirect water heating by means of a heat exchanger, the mathematical modelling of this type of systems is more complex. Dynamic material and energy balances for the reactor and the heating–cooling loop system are given as follows (all variables are described in the nomenclature section and in Tables 2, 3 and 4).

$$\frac{\mathrm{d}N_i}{\mathrm{d}t} = r_i + F_i, \quad i \in [A_1, A_2, A_1^*, A_2^*, \times B, B_p, B_f, D, E, F, G, \text{Aloph}], \tag{1}$$

$$\frac{\mathrm{d}V}{\mathrm{d}t} = \sum_{j=1}^{n_r} \frac{F_j M_j}{\rho_j}, \quad j \in [B_p, D], \tag{2}$$

$$\frac{\mathrm{d}T_r}{\mathrm{d}t} = \frac{-\Delta H_r(r_B + r_{B_p} + r_E)V - \sum_{j=1}^{n_r} F_j M_j C p_j (T_r - T_o) - U A (T_r - \bar{T}_j)}{\sum_{i=1}^{n} N_i M_i C p_i}, \tag{3}$$

Table 1
Polyurethane copolymerization mechanism

Isocyanate and polyol reactions	*Isocyanate and 1,4-butanediol reactions*
$A_1A_2 + B \xrightarrow{k_1} {}^*A_1A_2B - (E)$	$A_1A_2 + B' \xrightarrow{k_3} {}^*A_1A_2B - (E)$
$A_1A_2 + B \xrightarrow{k_2} {}^*A_1A_2B - (E)$	$A_1A_2 + B' \xrightarrow{k_4} {}^*A_1A_2B - (E)$
$-A_1^* + B \xrightarrow{k_1^*} -A_1B' - (E)$	$-A_1^* + B' \xrightarrow{k_3^*} -A_1B' - (E)$
$-A_2^* + B \xrightarrow{k_2^*} -A_2B' - (E)$	$-A_2^* + B' \xrightarrow{k_4^*} -A_2B' - (E)$
Isocyanate and hydroxyl functional groups	*Isocyanate and amine functional groups*
$A_1A_2 + B_{f-1} \xrightarrow{k_9} {}^*A_1A_2B_{f-2} - (E)$	$A_1A_2 + D \xrightarrow{k_5} {}^*A_1A_2D - (F)$
$A_1A_2 + B_{f-1} \xrightarrow{k_{10}} {}^*A_1A_2B_{f-2} - (E)$	$A_1A_2 + D \xrightarrow{k_6} {}^*A_1A_2D - (F)$
$-A_1^* + B_{f-1} \xrightarrow{k_9} -A_1B_{f-2} - (E)$	$-A_1^* + D \xrightarrow{k_5^*} -A_1D - (F)$
$-A_2^* + B_{f-1} \xrightarrow{k_{10}^*} -A_2B_{f-2}-$	$(E) - A_2^* + D \xrightarrow{k_6^*} -A_2D - (F)$
Allophanate functional groups production	*Isocyanate and urea functional groups reactions*
$A_2A_1 + E \xrightarrow{R_3k_1} M(+{}^*A_2)$	$A_2A_1 + F \xrightarrow{k_7} G(+{}^*A_2)$
$A_1A_2 + E \xrightarrow{R_3k_2} M(+{}^*A_1)$	$A_1A_2 + F \xrightarrow{k_8} G(+{}^*A_1)$
$-A_1^* + E \xrightarrow{R_3k_1^*} M$	$-A_1^* + F \xrightarrow{k_7^*} G$
$-A_2^* + E \xrightarrow{R_3k_2^*} M$	$-A_2^* + F \xrightarrow{k_8^*} G$

$$\frac{\mathrm{d}T_j^{\mathrm{in}}}{\mathrm{d}t} = \frac{Q_{cw}}{V_{\mathrm{loop}}}(T_j^{\mathrm{out}} - T_j^{\mathrm{in}}) - \frac{Q_{\mathrm{new}}}{V_{\mathrm{loop}}}(T_j^{\mathrm{out}} - T_{\mathrm{new}}) + \frac{\lambda_s F_s}{\rho_{cw} C_{p_{cw}} V_{\mathrm{loop}}}, \tag{4}$$

$$\frac{\mathrm{d}T_j^{\mathrm{out}}}{\mathrm{d}t} = \frac{Q_{cw}}{V_j}(T_j^{\mathrm{in}} - T_j^{\mathrm{out}}) + \frac{UA(T_r - \bar{T}_j)}{\rho_{cw} C_{p_{cw}} V_j}, \tag{5}$$

where $\bar{T}_j$ is the average jacket temperature given by

$$\bar{T}_j = \frac{T_j^{\mathrm{in}} + T_j^{\mathrm{out}}}{2}, \tag{6}$$

conversion of monomers at time t is obtained from

$$x_j = \frac{N_j(0) + \int_0^t F_j(t)\,\mathrm{d}t - N_j(t)}{N_j(0) + \int_0^t F_j(t)\,\mathrm{d}t}, \quad j \in [A_1, B_p, B, D], \tag{7}$$

The nonlinear step-growth copolymerization reaction rates are:

$$r_{A_1} = -k_1[A_1]([B] + R_3[E]) - k_3[A_1][B_p] - k_9[A_1][B_f] - k_5[A_1][D] - k_7[A_1][F], \tag{8}$$

$$r_{A_2} = -k_2[A_2]([B] + R_3[E]) - k_4[A_2][B_p] - k_{10}[A_2][B_f] - k_6[A_2][D] - k_8[A_2][F], \tag{9}$$

$$r_{A_1^*} = -k_2[A_2][B] + k_4[A_2][B_p] + k_6[A_2][D] + R_3k_2[A_2][E] + k_8[A_2][F] + k_{10}[A_2][B_f] - k_1^*[A_1^*][B] - R_3k_1^*[A_1^*][E] - k_3^*[A_1^*][B_p] - k_5^*[A_1^*][D] - k_7^*[A_1^*][F] - k_9[A_1^*][B_f], \tag{10}$$

$$r_{A_2^*} = k_1[A_1][B] + k_3[A_1][B_p] + k_5[A_1][D] + R_3k_1[A_1][E] + k_7[A_1][F] + k_9[A_1][B_f] - k_2^*[A_2^*][B] - R_3k_2^*[A_2^*][E] - k_4^*[A_2^*][B_p] - k_6^*[A_2^*][D] - k_8^*[A_2^*][F] - k_{10}[A_2^*][B_f], \tag{11}$$

$$r_B = -(k_1[A_1] + k_2[A_2])[B] - k_1^*[A_1^*][B] - k_2^*[A_2^*][B], \tag{12}$$

$$r_{B_p} = -(k_3[A_1] + k_4[A_2])[B] - k_1^*[A_1^*][B] - k_2^*[A_2^*][B], \tag{13}$$

$$r_{B_f} = -(k_9[A_1] + k_4[A_2])[B_p] - k_3^*[A_1^*][B_p] - k_4^*[A_2^*][B_p], \tag{14}$$

$$r_D = -(k_5[A_1] + k_6[A_2])[D] - k_5^*[A_1^*][D] - k_6^*[A_2^*][D], \tag{15}$$

$$r_E = (k_1[A_1] + k_2[A_2])[B] + k_1^*[A_1^*][B] + k_2^*[A_2^*][B] + (k_3[A_1] + k_4[A_2])[B_p] + k_3^*[A_1^*][B_p] + k_4^*[A_2^*][B_p] - R_3[E]\{(k_1[A_1] + k_2[A_2]) + k_1^*[A_1^*] + k_2^*[A_2^*]\}, \tag{16}$$

$$r_F = (k_5[A_1] + k_6[A_2])[D] + k_5^*[A_1^*][D] + k_6^*[A_2^*][D] - [F]\{(k_7[A_1] + k_8[A_2])\} + k_7^*[A_1^*] + k_8^*[A_2^*], \tag{17}$$

$$r_{\text{Aloph}} = R_3[E]\{(k_1[A_1] + k_2[A_2]) + k_1^*[A_1^*] + k_2^*[A_2^*]\}, \tag{18}$$

$$r_G = [F]\{(k_7[A_1] + k_8[A_2]) + k_7^*[A_1^*] + k_8^*[A_2^*]\}. \tag{19}$$

The copolymerization kinetic mechanism is presented in Table 1. Semi-batch reactor and heating–cooling system design and operation parameters are shown in Table 2, while reaction rate constants and required physical data are shown in Table 3.

The calculation of the number average molecular weight (M_n), is carried out from its definition, in terms of initial mass and moles of molecules consumed at a given time, Eq. (53) in Vivaldo-Lima et al. (2004). Calculation of the weight average molecular weight M_w is carried out using the Macosko-Miller methodology, represented by Eqs. (52)–(100) in Vivaldo-Lima et al. (2004).

Table 2
Reactor design and operation parameters

Jacket volume, V_j	300 L
Loop residence time, t_{loop}	2 min
Loop cooling water flowrate, Q_{cw}	200 L/min
Loop inlet cooling water temperature, T_{new}	293.15 K
Steam specific latent heat, λ_s	597.2 kcal/kg
Feedstream temperature, T_o	293.15 K
Reactor heat-transfer area, A	27.2 m^2
Reactor diameter, d_r	3 m^2
Heat of reaction, $-\Delta H_r$	−22,100 kcal/kgmol
Global heat transfer coefficient, U	1.15 kcal/(m^2 min K)
Cooling water density, ρ_{cw}	1 kg/L
Cooling water heat capacity, Cp_{cw}	1 kcal/(kg K)

3. Dynamic optimization formulation

The SDO approach provides a way to compute optimal dynamic policies (i.e., temperature, initiator feed rates) for batch and semi-batch reactors even in presence of challenging nonlinear behavior. In this approach, the computation of optimal policies is reduced to the solution of a nonlinear optimization problem (Biegler, 1992). The solution of such problem will provide values of the decision variables (i.e., the manipulated variables) that drive the system towards the optimality region, whose location is dictated by the desired objective function and constraints.

In order to solve dynamic optimization problems, three main approaches have been suggested: (a) iterative methods based on variational conditions, (b) feasible path nonlinear programming methods and (c) simultaneous nonlinear programming (SDO) methods. An excellent review on the subject topic was presented in (Biegler, 1992).

In the SDO approach both the manipulated and controlled variables are discretized along the expected solution trajectory. This leads to a nonlinear programming problem whose solution provides the full manipulated and controlled time variable profiles. Due to the fact that fast variations in the controlled and manipulated variables might arise, the whole solution space is commonly divided into time intervals called finite elements. Inside each finite element the differential–algebraic equations are satisfied at Radau collocation points. This approach corresponds to a fully implicit Runge–Kutta method with high-order accuracy and stability properties. Other methods based on different collocation discretizations (Betts, 2001) and backward difference formulae (Jockenhaevel et al., 2003) have also been used.

Table 3
Kinetic constants and species physical data

Kinetic constants	Physical data	
$R_3 = 0.00263$	Diisocyanate molecular weight, M_{A_1}	250 kg/kg mol
$k_1 = 5.1 \times 10^3 e^{-4900/T}$	Polyol molecular weight, M_B	2500 kg/kg mol
$k_3 = 1.43523 \times 10^7 e^{-6475/T}$	1,4-Butanediol molecular weight, M_{B_p}	90 kg/kg mol
$k_1^* = 1.2058 \times 10^8 e^{-8135/T}$	Multiol molecular weight, M_{B_p}	92 kg/kg mol
$k_3^* = 1.486e^{-1500/T}$	Diamine molecular weight, M_D	158 kg/kg mol
$k_2 = k_1$	Urethane molecular weight, M_E	59 kg/kgmol
$k_4 = k_3$	Urea molecular weight, M_F	58 kg/kgmol
$k_5 = 2k_3$	Allophanate molecular weight, M_{Alloph}	101 kg/kg mol
$k_6 = k_5$	Biuret molecular weight, M_G	100 kg/kg mol
$k_7 = R_3 k_1$	Isocyanate heat-capacity, $C_{p_{A_1}}$	0.1342 kcal/kg min
$k_8 = k_7$	Polyol heat-capacity, C_{p_B}	0.2623 kcal/kg min
$k_2^* = k_1^*$	1,4-Butanediol heat-capacity, $C_{p_{B_p}}$	0.0231 kcal/kg min
$k_4^* = k_3^*$	Diamine heat-capacity, C_{p_D}	0.2200 kcal/kg min
$k_5^* = 2k_3^*$	Isocyanate density, ρ_{A_1}	1410 kg/L
$k_6^* = k_5^*$	Polyol density, ρ_B	910 kg/L
$k_7^* = R_3 k_1^*$	1,4-Butanediol density, ρ_{Bp}	1064 kg/L
$k_8^* = k_7^*$	Diamine density, ρ_D	1320 kg/L
$k_9 = k_{10} = k_9^* = k_{10}^* = 0$		

T is in K.

3.1. Formulation

A common dynamic optimization scenario for batch and semi-batch reactors consists in finding optimal manipulated variables time profiles minimizing batch time, which lead to obtain a product of desired properties. The minimum time transition policy requires setting the following optimization problem (Flores-Tlacuahuac et al., 2004a)

$$\min \int_0^{\theta} \left\{ \mathbf{W}\|\mathbf{z}_1(t) - \hat{\mathbf{z}}_1(t)\|^2 + w_f\|F_{Bp}(t) - \hat{F}_{Bp}\|^2 + w_s\|F_s(t) - \hat{F}_s\|^2 + w_q\|Q_{\text{new}}(t) - \hat{Q}_{\text{new}}\|^2 \right\} \mathrm{d}t \quad (20)$$

s.t. semi-explicit DAE model:

$$\frac{\mathrm{d}\mathbf{z}(t)}{\mathrm{d}t} = \mathbf{F}(\mathbf{z}(t), \mathbf{y}(t), \mathbf{u}(t), t, \mathbf{p}), \quad (21)$$

$$0 = \mathbf{G}(\mathbf{z}(t), \mathbf{y}(t), \mathbf{u}(t), t, \mathbf{p}). \quad (22)$$

Initial conditions:

$$\mathbf{z}(0) = \mathbf{z}^0. \quad (23)$$

Bounds:

$$\begin{aligned} &\mathbf{z}^L \leqslant \mathbf{z}(t) \leqslant \mathbf{z}^U, \\ &\mathbf{y}^L \leqslant \mathbf{y}(t) \leqslant \mathbf{y}^U, \\ &\mathbf{u}^L \leqslant \mathbf{u}(t) \leqslant \mathbf{u}^U, \\ &\mathbf{p}^L \leqslant \mathbf{p} \leqslant \mathbf{p}^U, \end{aligned} \quad (24)$$

where $\mathbf{F}$ is the vector of right-hand sides of differential equations in the DAE model, $\mathbf{G}$ is the vector of algebraic equations, assumed to be index one, $\mathbf{z}$ is the differential state vector, $\mathbf{z}^0$ are the initial values of $\mathbf{z}$, $\mathbf{y}$ is the algebraic state vector, $\mathbf{u}$ is the control profile vector, $\mathbf{p}$ is a time-independent parameter vector, and θ is the transition horizon. The superscript "$\wedge$" stands for the desired end value. In the objective function of the above dynamic optimization formulation, $\mathbf{z}_1$ stands for the vector which contains those states that are part of the objective function. In our case $\mathbf{z}_1 = [M_w \;\; N_{A1} \;\; N_b]^{\mathrm{T}}$. $\mathbf{W}$ stands for a diagonal weighting matrix, where $\mathbf{W} = \mathrm{diag}([10^3 \;\; 10^5 \;\; 1])$, while w_f, w_s and w_q are weighting scalars employed to attain smooth control actions. After some trials, it was found that the following weighting values resulted in smooth control actions: $w_f = 10^3$, $w_s = w_q = 10^2$.

The DAE optimization problem is converted into an NLP by approximating state and control profiles by a family of polynomials on finite elements ($t_0 < t_1 < \cdots < t_{ne} = \theta$). Here, we use a monomial basis representation for the differential profiles, as follows:

$$\mathbf{z}(t) = \mathbf{z}_{i-1} + h_i \sum_{q=1}^{\text{ncol}} \Omega_q \left(\frac{t - t_{i-1}}{h_i} \right) \left. \frac{\mathrm{d}\mathbf{z}}{\mathrm{d}t} \right|_{i,q}, \quad (25)$$

where $\mathbf{z}_{i-1}$ is the value of the differential variable at the beginning of element i, h_i is the length of element i, $\mathrm{d}\mathbf{z}/\mathrm{d}t_{i,q}$ is the value of its first derivative in element i at the collocation point q, and Ω_q is the polynomial of order ncol, satisfying

$$\begin{aligned} &\Omega_q(0) = 0 \quad \text{for } q = 1, \ldots, \text{ncol}, \\ &\Omega_q'(\rho_r) = \delta_{q,r} \quad \text{for } q, r = 1, \ldots, \text{ncol}, \end{aligned}$$

where ρ_r is the location of the rth collocation point within each element. Continuity of the differential profiles is enforced by

$$\mathbf{z}_i = \mathbf{z}_{i-1} + h_i \sum_{q=1}^{\text{ncol}} \Omega_q \left(\frac{t - t_{i-1}}{h_i} \right) \left. \frac{\mathrm{d}\mathbf{z}}{\mathrm{d}t} \right|_{i,q}. \quad (26)$$

Here, Radau collocation points are used because they allow constraints to be set easily at the end of each element. In addition, the control and algebraic profiles are approximated using a similar monomial basis representation which takes the form

$$\mathbf{y}(t) = \sum_{q=1}^{\text{ncol}} \psi_q \left(\frac{t - t_{i-1}}{h_i} \right) y_{i,q}, \quad (27)$$

$$\mathbf{u}(t) = \sum_{q=1}^{\text{ncol}} \psi_q \left(\frac{t - t_{i-1}}{h_i} \right) u_{i,q}. \quad (28)$$

Here $y_{i,q}$ and $u_{i,q}$ represent the values of the algebraic and control variables, respectively, in element i at collocation point q. ψ_q is the Lagrange polynomial of order ncol satisfying

$$\psi_q(\rho_r) = \delta_{q,r} \quad \text{for } q, r = 1, \ldots, \text{ncol}.$$

From Eq. (25), the differential variables are required to be continuous throughout the time horizon, while the control and algebraic variables are allowed to have discontinuities at the boundaries of the elements. It should be mentioned that with representation (25), the bounds on the differential variables are enforced directly at element boundaries; however, they can be enforced at all collocation points by writing appropriate point constraints.

In addition, the integral objective function is approximated with Radau quadrature with ne finite elements and ncol quadrature points in each element. This leads to the following objective function:

$$\text{Min } \Phi = \sum_{i=1}^{\text{ne}} h_i \sum_{j=1}^{\text{ncol}} \omega_j \|\mathbf{z}(t_{i,j}) - \hat{\mathbf{z}}\|^2. \quad (29)$$

Finally, substitution of Eqs. (25)–(28) into Eqs. (20)–(24) leads to the following NLP.

$$\min_{\mathbf{x} \in \mathscr{R}^n} \quad f(\mathbf{x}) \quad (30)$$

$$\text{s.t.} \quad c(\mathbf{x}) = 0, \quad (31)$$

$$\mathbf{x}_L \leqslant \mathbf{x} \leqslant \mathbf{x}_U, \quad (32)$$

where $\mathbf{x} = ((\mathrm{d}z/\mathrm{d}t)_{i,q}, z_i, y_{i,q}, u_{i,q}, t, p)^{\mathrm{T}}$, $f : \mathscr{R}^n \longrightarrow \mathscr{R}$ and $c : \mathscr{R}^n \longrightarrow \mathscr{R}^m$.

3.2. Formulation and solution of the nonlinear program

The dynamic optimization formulation given in Eqs. (30)–(32) was implemented using the AMPL mathematical programming language (Fourer et al., 1993) and solved using the IPOPT algorithm (Waechter, 2002) for large-scale nonlinear programming. This algorithm follows a barrier approach, where the bound constraints (32) are replaced by logarithmic barrier terms which are added to the objective function to give

$$\min f(\mathbf{x}) - \mu \left(\sum_{i=1}^{n} \ln(x^{(i)} - x_L^{(i)}) + \sum_{i=1}^{n} \ln(x_U^{(i)} - x^{(i)}) \right) \tag{33}$$

$$\text{s.t.} \quad c(\mathbf{x}) = 0 \tag{34}$$

with a barrier parameter $\mu > 0$. Here, $x^{(i)}$ denotes the ith component of the vector $\mathbf{x}$. Since the objective function of this barrier problem becomes arbitrarily large as $x^{(i)}$ approaches either of its bounds, a local solution $\mathbf{x}_*(\mu)$ of this problem lies in the interior of this set, i.e., $\mathbf{x}_U > \mathbf{x}_*(\mu) > \mathbf{x}_L$. The degree of influence of the barrier is determined by the size of μ, and under certain conditions $\mathbf{x}_*(\mu)$ converges to a local solution $\mathbf{x}_*$ of the original problem (30)–(32) as $\mu \to 0$. Consequently, a strategy for solving the original NLP is to solve a sequence of barrier problems (33)–(34) for decreasing barrier parameters μ_l, where l is the counter for the sequence of subproblems. IPOPT follows a primal–dual approach and applies a Newton method to the resulting KKT conditions. Exact first and second derivatives for this method are provided automatically through the AMPL interface. More information on IPOPT can be found in Waechter and Biegler (2004).

4. Case studies and results

Optimal operation policies were sought for three different reactor operation scenarios. The main control objective is posed as to maximize the copolymer molecular weight for a fixed batch time, avoiding reaching the gelation point. The formation of a polymer network is a highly nonlinear phenomenon that severely complicates the optimization algorithm convergence to an even local optimal solution, since tiny changes in the decision variables might lead to an orders of magnitude increase of the weight average molecular weight. Industrially, it has been reported (Barksby et al., 2000) that batch-like operation leads to attain a low isocyanate conversion values if 1,4-butanediol is not initially loaded. Therefore, a promising way to enhance conversion may require the semi-batch addition of 1,4-butanediol. The potential manipulated variables are (depending upon the operation scenario) the cooling water (Q_{new}) and steam (F_s) flowrates, and the rates of addition of 1,4-butanediol and diamine. The operation conditions at the beginning of the polymerization are described in Table 4. This table also depicts the target values of the variables contained in the objective function definition.

Table 4
Initial values of the states that are part of the objective function and manipulated variables

Reactor volume, $V(0)$	4360 L
Loop inlet cooling water flowrate, $Q_{\text{new}}(0)$	0 L/min
Steam flowrate, $F_s(0)$	0 kg/min
Diisocyanate load, $N_A(0)$	6000 kg mol
Polyol load, $N_B(0)$	1200 kg mol
1,4 Butanediol feed flowrate, $F_{Bp}(0)$	0 kg mol/min
Diamine feed flowrate, $F_D(0)$	0 kg mol/min
$\hat{N}_{A1}$	900 kg mol
$\hat{N}_B$	0 kg mol
$\hat{F}_{pb}$	0 kg mol/min
$\hat{F}_s$	0 kg mol/min
$\hat{Q}_{\text{new}}$	0 kg mol/min

The initial value of the remaining states is zero. Also shown are the desired end values of states and manipulated variables.

Molecular weight development can be controlled by imposing restrictions to the 1,4-butanediol and diamine flowrates in such a way that, at the final batch time, hydroxyl and isocyanate groups are equal, that is, a final stoichiometric imbalance ratio (SIR) value of 1 is reached. If only 1,4-butanediol (B_p) and diamine (D) are considered as reactor feeds, the SIR is defined at time t as

$$\begin{aligned} \text{SIR}(t) &= \frac{[-\text{OH}]}{[-\text{NCO}]} \\ &= \frac{N_B(0) + N_{Bp}(0) + \int_0^t F_{Bp}(t)\,\mathrm{d}t + N_D(0) + \int_0^t F_D(t)\,\mathrm{d}t}{N_{A_1}(0) + N_{A_2}(0)}, \end{aligned} \tag{35}$$

For the purely batch case in which 1,4-butanediol is initially loaded to the reactor among polyol and isocyanate loads and the diamine presence is neglected, the SIR is no longer function of time and is reduced to

$$\text{SIR} = \frac{[-\text{OH}]}{[-\text{NCO}]} = \frac{N_B(0) + N_{Bp}(0)}{N_{A_1}(0) + N_{A_2}(0)}. \tag{36}$$

Since full discretization of F_{Bp} and F_D is needed over the entire time horizon, integral terms in the SIR expression might be replaced, in order to avoid Radau quadrature approximation, by a pair of pseudo-states with their dependence over time represented by a pair of ordinary differential equations

$$\int_0^t F_{Bp}(t) = N_{Bp}^{\text{in}}(t), \tag{37}$$

$$\int_0^t F_D(t) = N_D^{\text{in}}(t), \tag{38}$$

replacing in Eq. (35),

$$\mathrm{SIR}(t) = \frac{[-\mathrm{OH}]}{[-\mathrm{NCO}]} = \frac{N_B(0) + N_{Bp}(0) + N_{Bp}^{\mathrm{in}}(t) + N_D(0) + N_D^{\mathrm{in}}(t)}{N_{A_1}(0) + N_{A_2}(0)} \quad (39)$$

with

$$\frac{\mathrm{d}N_{Bp}^{\mathrm{in}}}{\mathrm{d}t} = F_{Bp}(t), \quad (40)$$

$$\frac{\mathrm{d}N_D^{\mathrm{in}}}{\mathrm{d}t} = F_D(t), \quad (41)$$

$$N_{B_p}^{\mathrm{in}}(0) = N_D^{\mathrm{in}}(0) = 0. \quad (42)$$

It is worth remarking the difference between Eqs. (35) and (36). Eq. (35) will be used as restriction only for cases in which 1,4-butanediol and both 1,4-butanediol and diamine feed rates are allowed. Eq. (36) will be used only in the purely batch case where 1,4-butanediol is initially loaded.

After adding the algebraic equations required for molecular weight computation, the final mathematical model obtained consists on a set of 17 ordinary-differential and 72 algebraic equations. In all analyzed cases, 3 collocation points and 20 finite elements where used for temporal discretization, leading to an average of 1250 variables and 1200 constraints. It should be stressed that for today standards, the underlying optimization program looks like a rather small size nonlinear optimization problem. Although it is difficult to define precisely the size of a nonlinear optimization problem to be considered as a "large-scale" problem, presently this statement would probably indicate nonlinear programs with around 1–2 $\times$ 10^6 variables. Such large-scale problems can only be solved by exploiting the problem structure (i.e., sparsity). Actually, what makes difficult to solve the addressed polyurethane dynamic optimization problem, is not the number of variables and constraints involved, but instead the high nonlinear behavior embedded in the model description of the reactor performance.

4.1. Batch case

In this case, only cooling water (Q_{new}) and steam (F_s) flowrates are considered as the manipulated variables for control purposes, and are used to drive the reactor temperature trajectory over the batch operation. Initial amounts of isocyanate, polyol and 1,4-butanediol are loaded into the reactor, and diamine addition is not considered. Since gel formation ($M_w \to \infty$) is highly dependent upon the temperature policy and the reaction time, some open-loop profiles were obtained by simulation in order to fix a suitable time span. Therefore, different temperature policies were obtained, maximizing M_w by sequential computations, avoiding the onset of the gelation point. A fixed batch time is suitable for comparing results with subsequent cases analyzed in order to determine the best proposed operation scheme. In order to yield the desired control objective, the objective function (see Eq. (20)) is expressed in terms of the isocyanate, polyol and 1,4-butanediol molar contents, which are the most representative species that modify the molecular weight profile and is penalized by deviations from the final desired molecular weight value.

In Fig. 2, reactor temperature and jacket temperatures, cooling water and steam feed rates optimal profiles for the batch reactor are presented. The control objective was to reach a final molecular weight of 1×10^5 , as shown in Fig. 3. The onset of the gelation point was successfully avoided, and the reaction might be controlled by manipulating the reactor temperature profile only. It is worth mentioning the exponential-like behavior of the molecular weight profile reaching high-molecular weights during the final instants of the batch time, highlighting the fast growing of the polymer molecules, which could ultimately reach an infinite size (i.e., the gelation point), if the reaction was allowed to proceed further.

The temperature profile consists of three operation stages. In the first stage (initial heating phase), reactor temperature is raised up to 320 K and is then dropped down to 300 K keeping a constant value (isothermal phase) during 95 min, and finally is raised rapidly again near to 360 K to achieve the desired molecular weight value.

The major extent of isocyanate, polyol and 1,4-butanediol conversions occurs during the initial heating phase, while almost negligible isocyanate and polyol conversions are obtained during the isothermal and the final heating stages. However, a considerable amount of 1,4-butanediol reacts during these final stages. Although, it has been reported the formation of a gel molecule at high 1,4-butanediol conversion levels (Vivaldo-Lima et al., 2004), the computations demonstrate that this undesired behavior might be avoided by employing the calculated optimal temperature profile.

In order to show the high sensitivity of the polyurethane properties to small variations in the decision variables, an optimal solution was sought for a desired molecular weight value of 1.5×10^5. In Figs. 4 and 5, profiles for achieving a final molecular weight value 1.5×10^5 are presented. Isocyanate, polyol and 1,4-butanediol conversion profiles are essentially the same as in the previous case. However, a longer isothermal stage is obtained, compared to the first case. This situation highlights the high sensitivity of the molecular weight profile to small changes in the temperature profile. The difference between this two cases might be explained by analyzing the polyol conversion profiles. At a reaction time of 300 min conversion values of 96% and 92% for the first and second cases, respectively, are obtained. This means that the polyol conversion profile is retarded for the second case as a result of a longer isothermal polymerization stage, improving polymer chains extension and allowing more polyol units to react during the final reaction time and, consequently, obtaining a higher molecular weight. From an operation point of view, is clear that specifying a larger end MWD value (in the same fixed period of

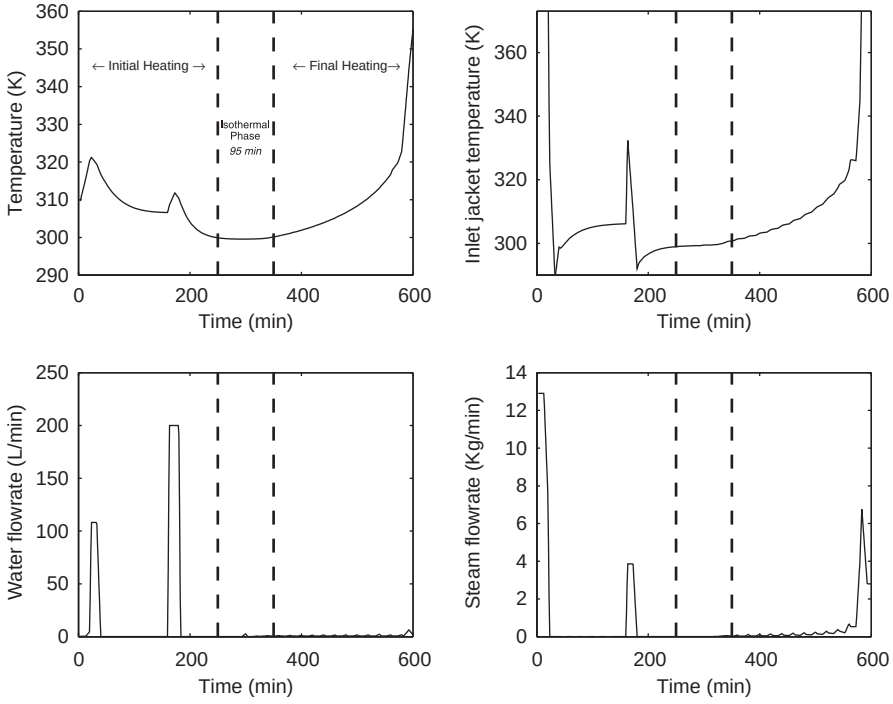

Fig. 2. Reactor and jacket temperature, cooling water and steam optimal profiles for batch operation ($M_w = 1 \times 10^5$).

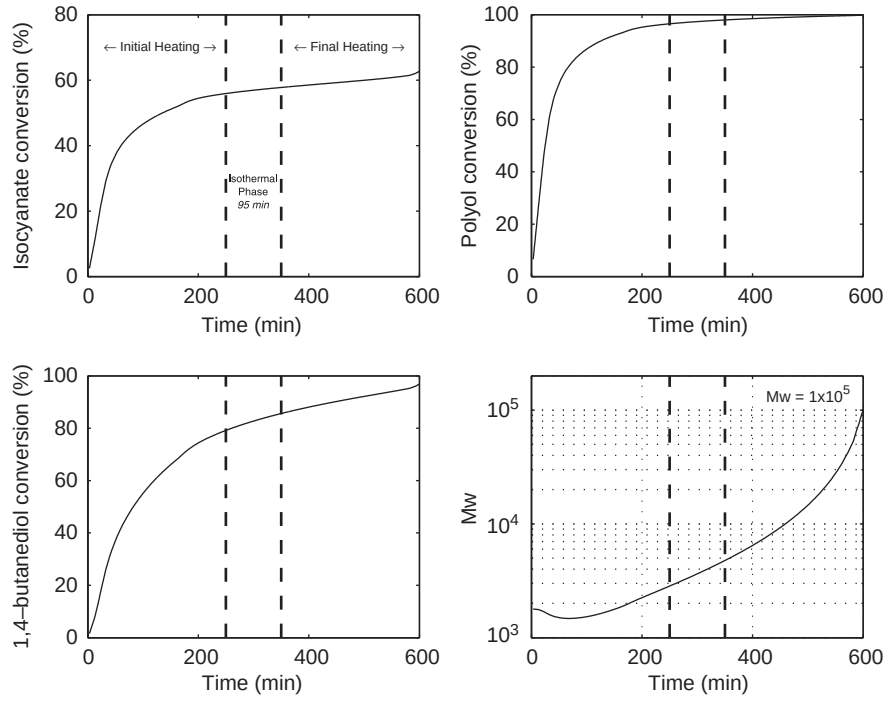

Fig. 3. Isocyanate, polyol and 1,4-butanediol conversion and weight-average molecular weight profiles for batch operation ($M_w = 1 \times 10^5$).

time), forces the reactor to employ larger and early control actions to meet the target MWD value.

No further molecular weight increase was obtained for the batch operation mode, mainly due to computational difficulties. In Fig. 6, temperature and molecular weight profiles are presented for the particular case in which a final molecular weight of 2×10^5 was sought. The proximity to the gelation point is evident at around 280 min of reaction time, leading to a dramatic jump between 10^4 and -11×10^4 values. The onset of the gelation point might be one of the reasons for

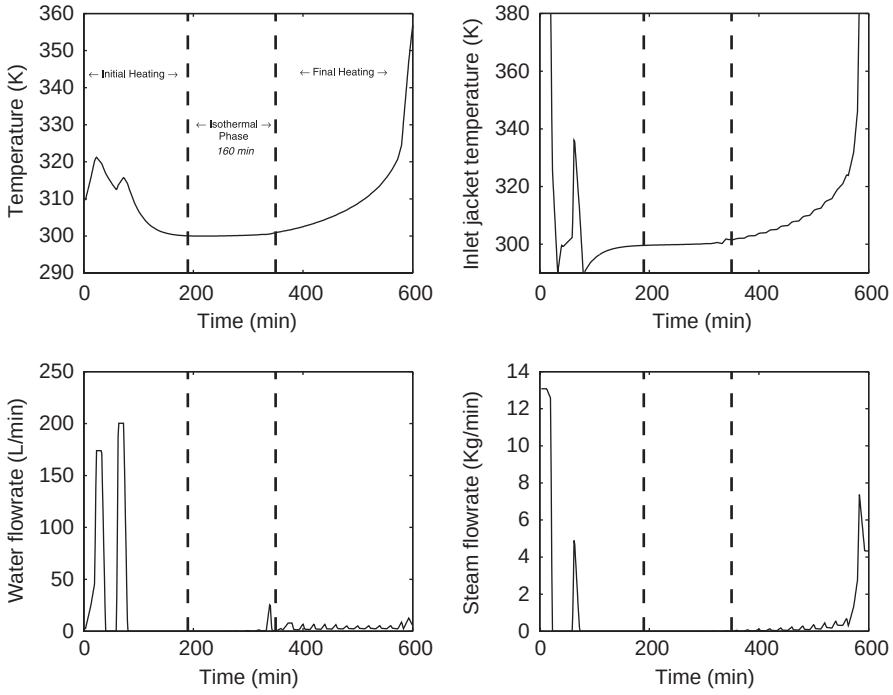

Fig. 4. Reactor and jacket temperature, cooling water and steam profiles for batch operation ($M_w = 1.5 \times 10^5$).

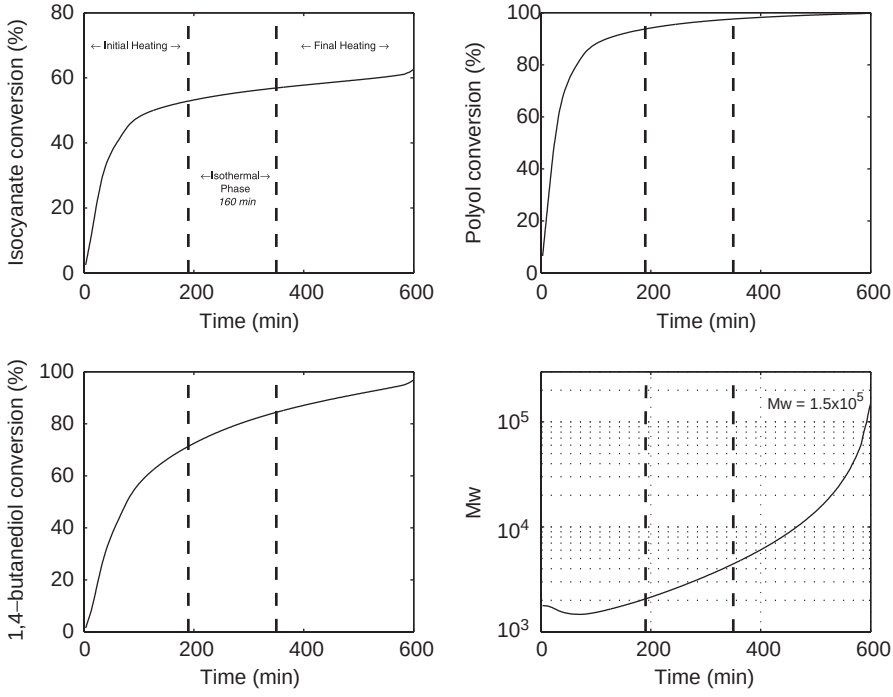

Fig. 5. Isocyanate, polyol and 1,4-butanediol conversion and weight-average molecular weight profiles for batch operation ($M_w = 1.5 \times 10^5$).

convergence problems. In the proximity of the onset of the gel effect an extremely high sensitivity between molecular weight profiles and reactor operating conditions exists, leading to orders of magnitude changes in the final molecular weight profile for small changes in the decision variables values. Desired molecular weight values cannot be achieved because of the proximity to the gelation point, probably during the final reaction time or even before. It should be stressed that the negative M_w values, shown in Fig. 6, do not have any physical meaning, since the Macosko–Miller

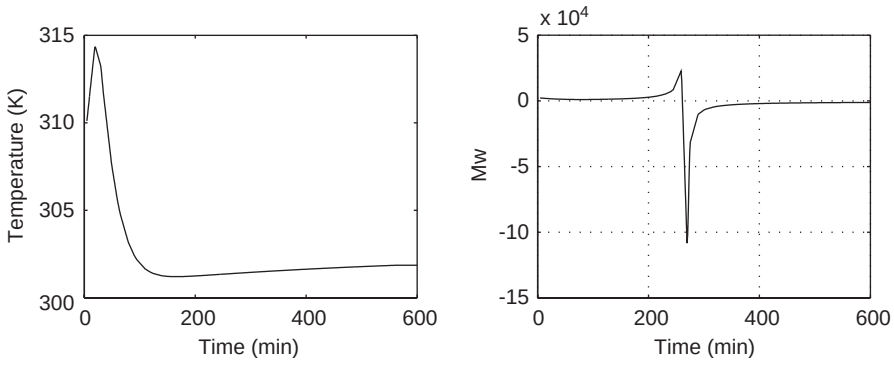

Fig. 6. Temperature and M_w profiles showing the effect of gel formation on convergence.

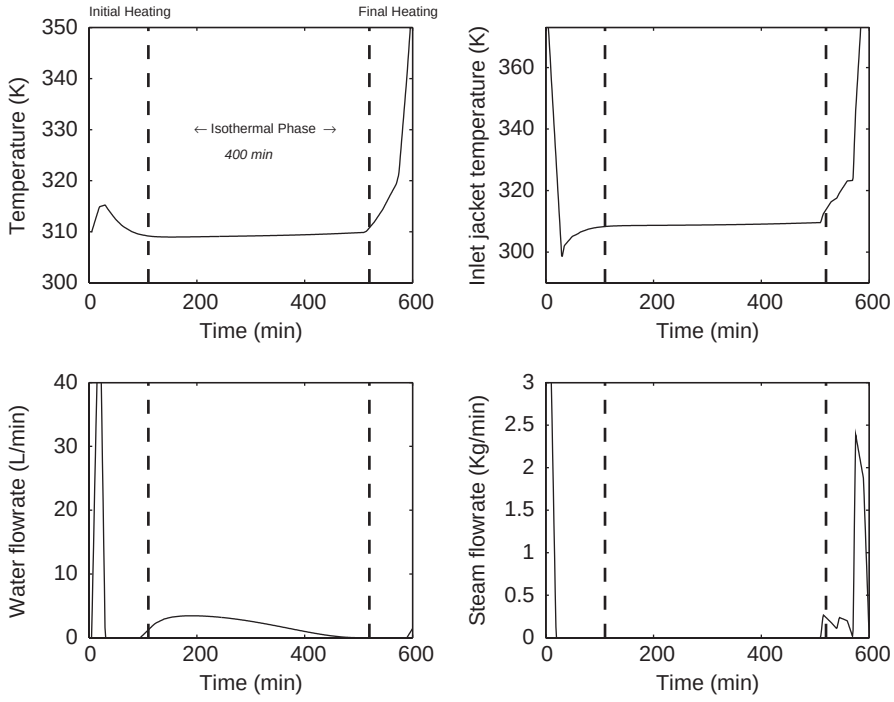

Fig. 7. Reactor and jacket temperature, cooling water and steam profiles for semi-batch operation with 1,4-butanediol added in semi-batch form ($M_w = 1 \times 10^5$).

model is valid only during the pre-gelation period. Those M_w negative values were included just to show that near the onset of the gelation point, the numerical optimization algorithm fails to find a feasible solution. In summary, reactor temperature profile control alone is not good enough to effectively restrict the onset of the gelation point, failing to obtain large molecular weight values.

4.2. Semi-batch case (1,4-butanediol addition)

Higher molecular weights can be obtained by manipulating the diol conversion profile, since it might modify, to some extent, the molecular weight profile. Therefore, in addition to the manipulation of both water and steam flowrates, the rate of addition of 1,4-butanediol was also manipulated. For this case, the same total initial load of 1,4-butanediol than for the batch case is fed during the semi-batch operation, such that the final SIR restriction remains satisfied.

In Figs. 7–9, profiles for the reactor and jacket temperatures as well as isocyanate, polyol (high-molecular-weight diol) and diol (low-molecular-weight diol) conversion are shown. In this case a final weight average molecular weight of 1×10^5 is sought in order to compare the profiles with the profiles previously obtained for the purely batch case.

Isocyanate and polyol conversion profiles are similar to those obtained in the batch case, but they are slightly slower. However, the diol conversion profile presents some differences. The conversion level is kept under 80% for the first 300 min of operation. This behavior can be understood if the reactor temperature profile is considered. The isothermal

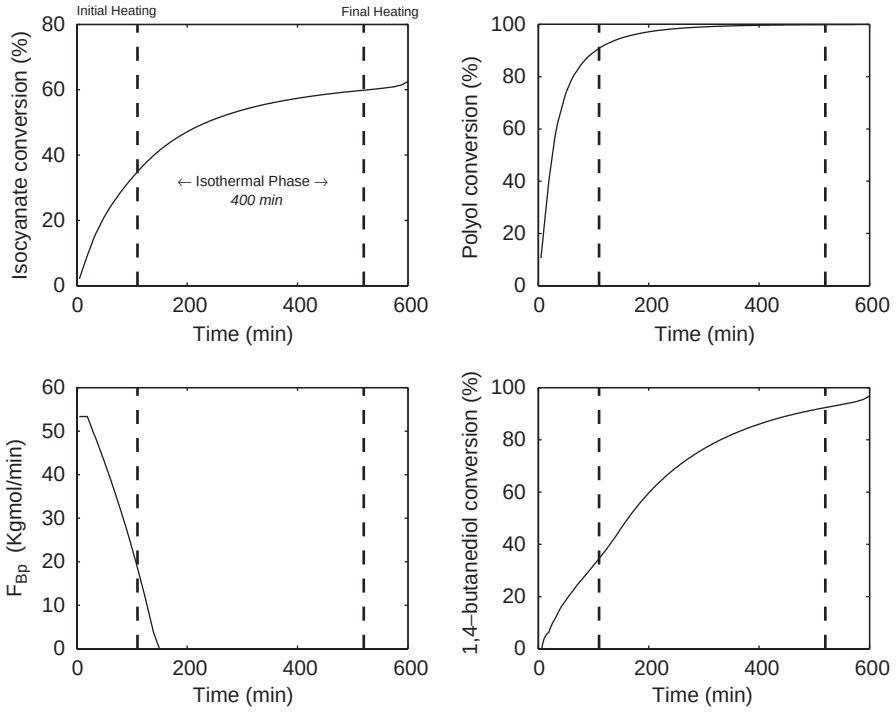

Fig. 8. Isocyanate, polyol and 1,4-butanediol conversion and 1,4-butanediol feed rate profiles for semi-batch operation with 1,4-butanediol added in semi-batch form ($M_w = 1 \times 10^5$).

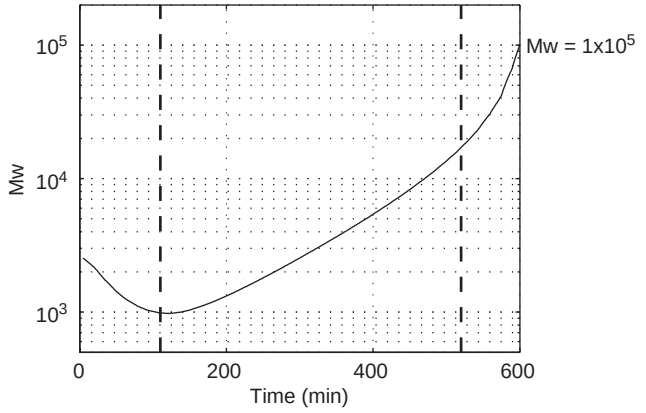

Fig. 9. Weight-average molecular weight profile for semi-batch operation with 1,4-butanediol added in semi-batch form ($M_w = 1 \times 10^5$).

stage has been extended over 400 min of the total polymerization time. This lower temperature profile compensates for the time invested on diol addition at the beginning of the operation, allowing the total consumption of diol units at the end of the batch time. Some differences are encountered in the molecular weight as well. During the diol addition stage (0–160 min), a remarkable molecular weight decrease is observed because of the addition of a low-molecular-weight agent. However, this 1,4-butanediol addition policy allows a better distribution of the isocyanate and polyol units giving rise to a smoother molecular weight profile. The final desired molecular weight is obtained by a fast increase of reactor temperature up to 350 K at the final heating stage, and also considering that the diol reacts faster than the polyol, thus providing a good mix of smoother increase of M_w due to an increase of free volume, followed by a period of sharper increase. Avoidance of the gelation point is easier under this operating scheme since diol and temperature policies have a strong effect on polymer properties allowing a more flexible polymer properties control scenario. As far as the operation of the semi-batch reactor is concerned, it is clear that the sluggish response shown by the semi-batch operation is due to the reduced amount of both cooling and heating utilities. The slower semi-batch reactor response may also be explained by recalling that sometimes (under adequate operating conditions) the dynamic reactor composition response tends to be slower than the pure dynamic thermal effects. Therefore, a combination of both types of dynamic responses is responsible for the slow response displayed by the semi-batch operation mode. The semi-batch operation strategy also diminished the computational complexity when solving the underlying nonlinear optimization problem. A notable decrease in the optimization algorithm CPU time and iterations is obtained for the semi-batch case. For instance, for the purely batch case, up to 1712 iterations and 516 CPU seconds were needed for achieving convergence. In contrast, for the semi-batch case, only 548 iterations and 399 s were needed. All the CPU times and IPOPT performance were obtained using a 1.5 GHz PC running the Linux operating system.

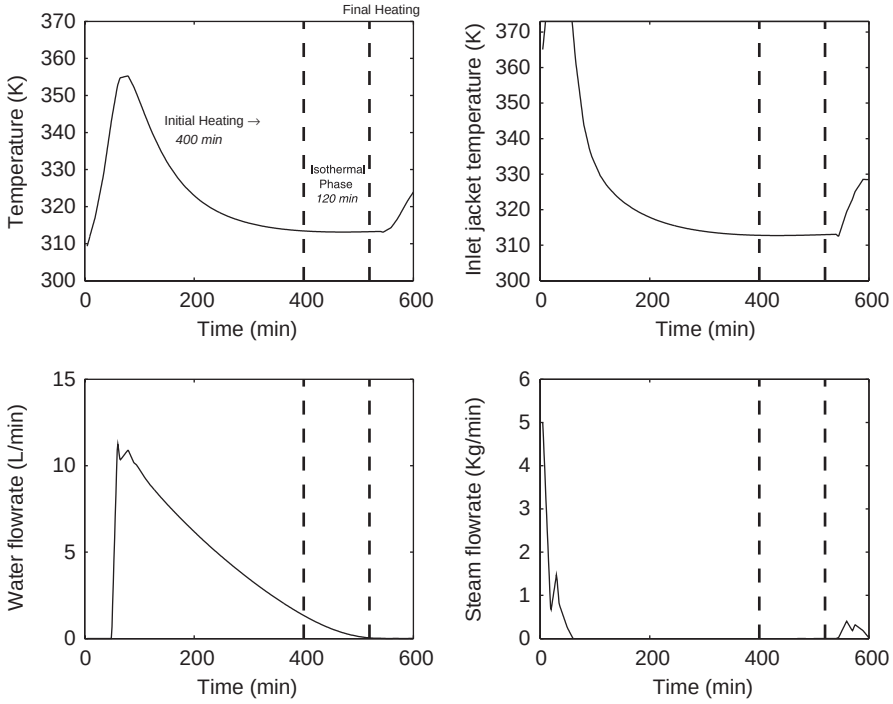

Fig. 10. Reactor and jacket temperature, cooling water and steam profiles for semi-batch operation with 1,4-butanediol added in semi-batch form ($M_w = 2 \times 10^5$).

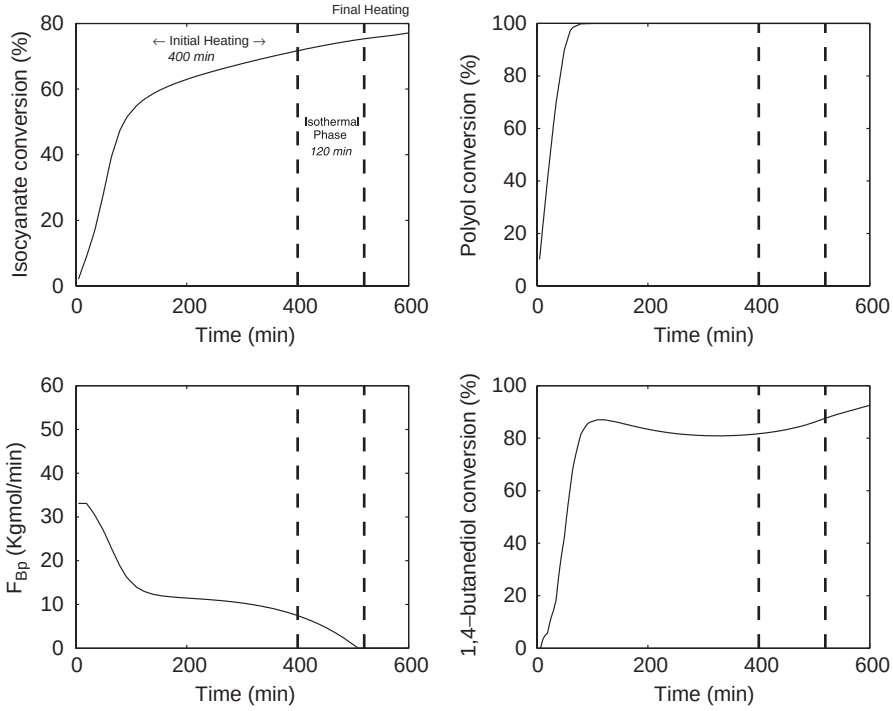

Fig. 11. Isocyanate, polyol and 1,4-butanediol conversion and 1,4-butanediol feed rate profiles for semi-batch operation with 1,4-butanediol added in semi-batch form ($M_w = 2 \times 10^5$).

Interesting results are obtained if higher molecular weight values are sought (Figs. 10–12). If the desired final molecular weight is increased to 2×10^5, a dramatic change is obtained for the temperature and diol addition policies. The initial heating stage is now characterized by a fast increase in the reactor temperature up to 355 K followed by a fast

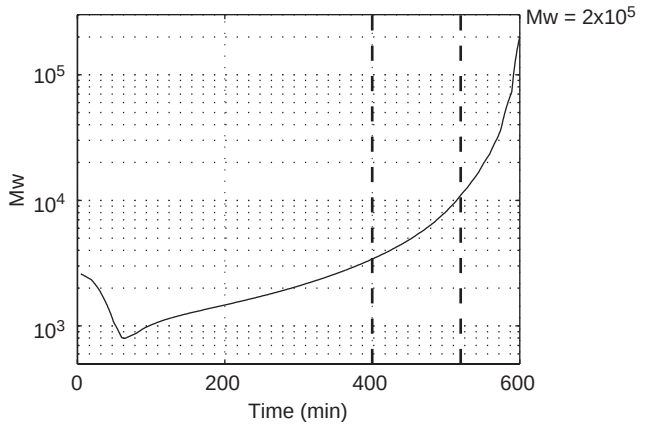

Fig. 12. Weight-average molecular weight profile for semi-batch case with 1,4-butanediol added in semi-batch form ($M_w = 2 \times 10^5$).

decrease down to 310 K. This stage is extended for over 400 min, while the isothermal stage is shortened to 120 min, and a small increase up to 320 K is accomplished in the final heating stage.

Diol addition is extended until the final hours of the polymerization, obtaining a fast increase of diol conversion in the first 100 min of operation and sustaining this conversion level over the rest of the operation. A higher isocyanate final conversion is obtained as consequence, reaching about 80% of total conversion. Polyol consumption is almost instantaneous. The remaining unreacted isocyanate should be consumed when the overall SIR approaches 1.0, close to the final time of addition of diol. The onset of the gelation point is efficiently avoided and the desired final polymer properties are obtained. From a dynamic point of view is clear, as in the pure batch case, that demanding a higher value of MWD (in the same fixed period of time) requires larger control actions. The fast response observed in the conversions is due to the large initial reactor temperature increase. The magnitude of the temperature increase is enough to rise the rate of reaction up to a large value speeding up the composition and reactor temperature dynamics. No convergence problems were encountered requiring 475 iterations and 483 CPU seconds. Nevertheless, no further improvement on the molecular weight was obtained. Although a diol addition policy might be able to modify the molecular weight profile, its influence is not strong enough to avoid the onset of the gelation point for the given batch time.

4.3. Semi-batch case (1,4-butanediol and diamine addition)

The use of amine "chain extenders" for polyurethane copolymerization is a common industrial practice. Amine compounds are more reactive species that polyols and low-molecular weight diols, and might lead to obtain smoother molecular weight profiles.

In this case, in order to improve the reactor performance, the simultaneous addition of 1,4-butanediol and diamine, together with the manipulation of both cooling water and steam flowrates, is considered. It is worth mentioning that

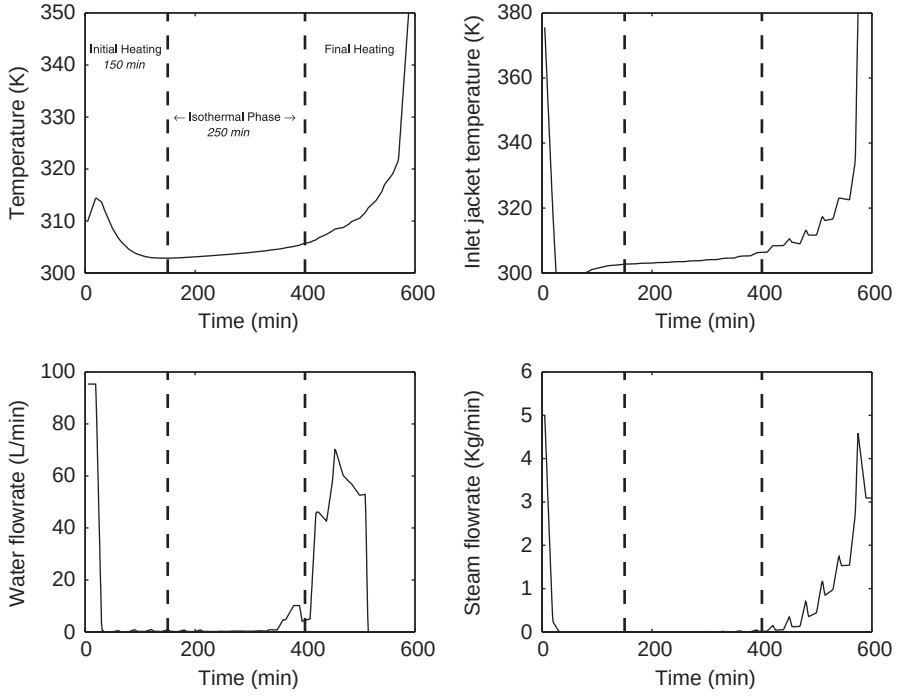

Fig. 13. Reactor and jacket temperature, cooling water and steam profiles for semi-batch operation with 1,4-butanediol and diamine simultaneous addition ($M_w = 1 \times 10^6$).

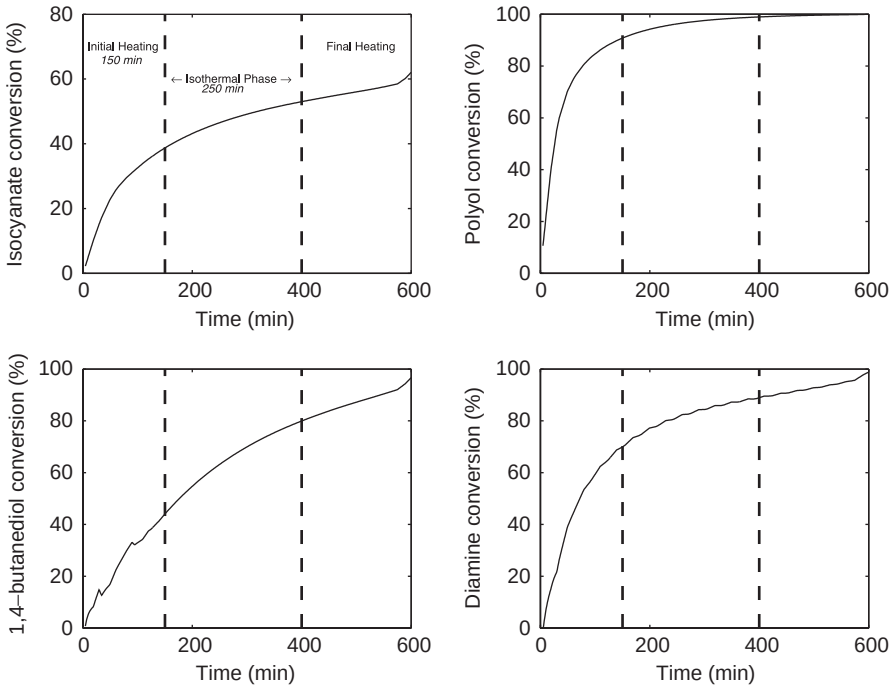

Fig. 14. Isocyanate, polyol, diamine and 1,4-butanediol conversion profiles for semi-batch case with 1,4-butanediol and diamine simultaneous addition ($M_w = 1 \times 10^6$).

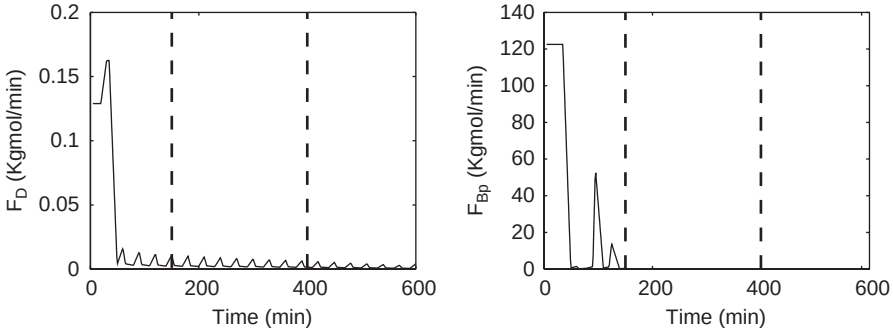

Fig. 15. 1,4-butanediol and diamine feed rate profiles for semi-batch case with 1,4-butanediol and diamine simultaneous addition ($M_w = 1 \times 10^6$).

the diamine fed to the reactor must be accounted for, in order to obtain a final SIR value comparable to the other cases. This means that some of the diol fed in the previous cases is replaced by the same molar amount of diamine, enhancing the reactive properties of the polymer chains. Since relatively large MWD values were already obtained by adding 1,4-butanediol, it was decided to force an order of magnitude increase in the MWD end value. Therefore, a final MWD value of 1×10^6 was specified at the end of the 600 min of the fixed operation period. In Figs. 13–16, profiles of reactor and jacket temperatures, isocyanate, polyol, diol and diamine conversions, diol and diamine feed rates and molecular weight are presented. A remarkable improvement in the weight average molecular weight profiles is accomplished. A final molecular weight of 1×10^6 is obtained for 600 min of operation. The temperature trajectory is similar to the one obtained for the batch cases. An isothermal stage of 250 min at 305 K and a final heating stage leading to a final temperature of 350 K are obtained. An evident difference opposed to the semi-batch addition of diol is the diol conversion profile. A smoother conversion profile is obtained allowing faster reaction with more available free volume. Although low diamine feed rates where obtained, the presence of the diamine in the polymerization system allows a better molecular weight control, reaching higher molecular weights, and contributing to avoid the onset of the gelation point. In fact, it is quite remarkable how small feedstream rates of diamine helped to attain large molecular weights, while avoiding the formation of a polymer network.

Diamine addition also makes the nonlinear optimization problem easier to solve. Although the introduction of an additional decision variable represents the inclusion of 60

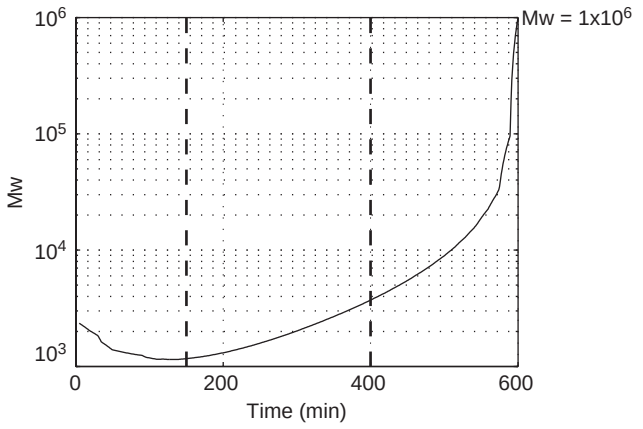

Fig. 16. M_W profile for semi-batch case with 1,4-butanediol and diamine simultaneous addition ($M_w = 1 \times 10^6$).

additional variables, convergence was achieved in less CPU time (363 seg) and iterations (277), compared to the other cases analyzed. This fact lead us to conclude that proper control of the copolymerization reactor will only be robust under this operation scheme. Diamine addition allows a more reliable and efficient process operation. From a process operability point of view, it is clear that the enhancement in the semi-batch reactor performance is due to the employment of additional manipulated variables, which have an important influence on the end MWD value.

5. Conclusions

In this work it has been shown that by applying tools and concepts from the process system engineering field, the polyurethane copolymerization reactor performance was greatly enhanced. In fact, it was possible to rise, by an order of magnitude, the MWD end value by just letting the reactor to operate in a semi-batch-like optimal form. Moreover, it is important to highlight that such large increase in MWD was achieved without running into polymer network formation problems.

Although previous polymerization reactor control and optimization studies are available in the literature (Elicabe and Meira, 1988), and some of our results are somehow expected based on the accumulated experience obtained by researchers and practitioners in the field, those studies are mostly targeted to free-radical polymerization systems, and are mainly of qualitative nature for step growth polymerization situations. None of them had addressed the optimization of polyurethane production reactors, using the dynamic optimization techniques used in this contribution.

In particular, it was found that the simultaneous addition of 1,4-butanediol and diamine, together with a proper reactor temperature profile, lead to a reliable operation scheme in which high-molecular-weight values are achieved without reaching the gelation point. Diamine and diol flowrates were kept at low values in order to avoid significant deviations from the mathematical model description of MWD valid for a batch reactor. Diamine addition allowed a decrease in CPU time and number of iterations compared to the other cases analyzed. This situation leads to conclude that the possibility of gel formation is an important limitation for efficient computation of optimal trajectories due to its highly nonlinear nature.

In this work, a robust and efficient dynamic optimization formulation was proposed for a polyurethane semi-batch copolymerization reactor under different operation scenarios. A highly complex probabilistic model, coupled to a detailed kinetic model, was used to compute copolymer molecular weight leading to some computational difficulties. Nevertheless, the dynamic optimization formulation was capable of obtaining optimal policies and was also employed to detect the presence of the formation of polymer network molecules.

Even in the face of the high complexity of the mathematical model, and the underlying dynamic optimization problem, only modest computation times where required. Therefore, real-time application of SDO for this type of copolymerization reactors looks like a real and feasible alternative to the operation of polyurethane reactors.

Notation

A	heat-transfer area, m^2
A_1, A_2	isocyanate functional groups concentration, mol/L
Alloph	allophanate functional group
B	concentration of hydroxyl functional groups bounded to the polyol, mol/L
B_p	concentration of hydroxyl functional groups bounded to the 1,4-butanediol molecule, mol/L
B_f	multiol molecule with f hydroxil functional groups
C_p	heat capacity, kcal/kg K
D	amine functional group concentration, mol/L
D_2	diamine molecule
E	urethane concentration, mol/L
F	urea functional group
G	biuret functional group, mol/L
k_i, k_i^*	kinetic rate constants, where superscript $*$ indicates reactivity of a functional group bound to a polymer molecule, L/mol min
M	allophanate functional group concentration, mol/L
M_n	number average molecular weight, kg/kmol
n	number of states
n_r	number of fed reactants
N	molar load, kmol
r	reaction rate, mol/L min
R_3	proportionality constant between rates of allophanate and urethane formation

SIR	stoichometric imbalance ratio
T_j^{in}	Cooling jacket input temperature, K
T_j^{out}	Cooling jacket output temperature, K
T_{new}	cooling water feedstream temperature, K
T_r	reactor temperature
V_{loop}	cooling/heating system volume, L
x	conversion

Greek letters

ΔH_r	heat of reaction, Kcal/mol
ρ	density, kg/L

References

Abel, O., Helbing, A., Marquardt, W., Zwick, H., Daszkowsky, T., 2000. Productivity optimization of an industrial semi-batch polymerization reactor under safety constraints. Journal of Process Control 10, 351–362.

Bahr, D., Pinto, J.C., 1991. Refractive index of solutions containing poly(vinyl acetate) and poly(methyl methacrylate). Journal of Applied Polymer Science 42, 2795–2809.

Barksby, N., Lawrey, B.D., Clift, S.M., 2000. Polyurethane and polyurethane/urea heat-cured and moisture-cured elastomers with improved physical properties. U.S. Patent 6,420,445.

Betts, J., 2001. Practical Methods for Optimal Control Using Nonlinear Programming. SIAM, Philadelphia, PA.

Biegler, L.T., 1992. Optimization strategies for complex process models. Advances in Chemical Engineering 18, 197–256.

Biegler, L.T., Grossman, I.E., 2004. Retrospective on optimization. Computational Chemical Engineering 28, 1169–1192.

Biegler, L.T., Cervantes, A.M., Waechter, A., 2002. Advances in simultaneous strategies for dynamic process optimization. Chemical Engineering Science 57(4), 575–593.

Boyd, S., Vandenberghe, L., 2004. Convex Optimization. Cambridge University Press, Cambridge.

Butala, D., Choi, K.Y., Fan, M.K.H., 1988. Multiobjective dynamic optimization of a semibatch free-radical copolymerization process with interactive CAD tools. Computational Chemical Engineering 12 (11), 1115–1127.

Catalgil-Giz, H., Giz, A., Alb, A., Reed, W.F., 2001. Absolute online monitoring of a stepwise polymerization reaction: polyurethane synthesis. Journal of Applied Polymer Science 82 (8), 2070–2077.

Chang, J.S., Lai, J.L., 1992. Computation of optimal temperature policy for molecular weight control in a batch polymerization reactor. Industrial Engineering and Chemical Research 31, 861–868.

Chien, D.C.H., Penlidis, A., 1990. On-line sensors for polymerization reactors. JMS-Review of Macromolecular Chemistry and Physics C30 (1), 1–42.

Clough, D.E., Masterson, P.M., Payne, S.R., 1978. Computational problems in the determination of control policies for batch polymerization. Proceedings of the Summer Computer Simulation Conference, July 1978, p. 279

Congalidis, J.P., Richards, J.R., 1998. Process control of polymerization reactors: an industrial perspective. Polymer Reaction Engineering 6 (2), 71–111.

Cuthrell, J.E., Biegler, L.T., 1987. On the optimization of differential–algebraic process systems. A.I.CH.E. Journal 33, 1257–1270.

Cuthrell, J.E., Biegler, L.T., 1989. Simultaneous optimization and solution methods for batch reactor control profiles. Computational Chemical Engineering 13 (1), 49–62.

Dimitratos, J., Elicabe, G., Georgakis, C., 1994. Control of emulsion polymerization reactors. A.I.Ch.E. Journal 40 (12), 1993–2001.

Dotson, N.A., Galvan, R., Laurence, R.I., Tirrel, M., 1996. Polymerization Process Modeling. VCH Publishers, Inc., New York.

Elicabe, G.E., Meira, G.R., 1988. Estimation and control in polymerization reactors. A review. Polymer Engineering and Science 28 (3), 121–135.

Flores-Tlacuahuac, A., Biegler, L.T., Saldivar-Guerra, E., 2004a. Optimal grade transitions in the HIPS polymerization process. Chemical Engineering Science, submitted for publication.

Flores-Tlacuahuac, A., Zavala-Tejeda, V., Vivaldo-Lima, E., 2004b. The bifurcation behavior of a polyurethane continuous stirred tank reactor. Computers and Chemical Engineering, submitted for publication.

Fourer, R., Gay, D.M., Kernighan, B.W., 1993. AMPL: A Modeling Language For Mathematical Programming. Thomson Publishing Company, Danvers, MA, USA.

Garcia-Rubio, L.H., MacGregor, J.F., Hamielec, A.E., 1982. Modeling and control of copolymerization reactors. In: Provder, T. (Ed.), Computer Applications in Applied Polymer Science. American Chemical Society Symposium Series, vol. 197, pp. 87–116.

Gill, P.E., Murray, W., Saunders, M.A., 1998. User's guide for SNOPT: a FORTRAN package for large-scale nonlinear programming. Technical Report, Department of Mathematics, University of California, San Diego, USA.

Hicks, J., Mohan, A., Ray, W.H., 1969. The optimal control of polymerization reactors. Canadian Journal of Chemical Engineering 47, 590.

Jockenhaevel, T., Biegler, L.T., Waechter, A., 2003. Dynamic optimization of the Tenessee Eastman process using the optcontrolcentre. Computational Chemical Engineering 27, 1513–1531.

Kammona, O., Chatzi, E.G., Kiparissides, C., 1999. Recent developments in hardware sensors for the on-line monitoring of polymerization reactions. JMS-Review of Macromolecular Chemistry and Physics C39 (1), 57–134.

Kiparissides, C., 1996. Polymerization reactor modeling: a review of recent developments and future directions. Chemical Engineering Science 51 (10), 1637–1659.

MacGregor, J.F., Penlidis, A., Hamielec, A.E., 1984. Control of polymerization reactors: a review. Polymer Process Engineering 2, 179–206.

Nogueira, E.S., Borges, C.P., Pinto, J.C., 2003. In-line monitoring and control of conversion and weight-average molecular weight of polyurethanes in solution step-growth polymerization based on near infrared spectroscopy and torquemetry. In: Proceedings of Polymer Reaction Engineering V, Engineering Foundation Conference, Quebec, Canada, May 2003.

Palanki, S., Vemuri, J., 2003. End-point optimization of batch chemical processes. Proceedings of the IEEE Conference on Decision and Control. Maui, Hawaii USA, pp. 4759–4764.

Penlidis, A., 1994. Polymer reaction engineering: from reaction kinetics to polymer reactor control. Canadian Journal of Chemical Engineering 72, 385–391.

Pontryagin, L.S., Boltyanskii, R., Gamkrelidge, R.V., Mishchenko, E., 1962. The Mathematical Theory of Optimal Processes. Interscience Publishers Inc., New York.

Ray, W.H., 1989. Computer-aided design, monitoring, and control of polymerization processes. In: Polymer Reaction Engineering. VCH Publishers, New York, pp. 105–122.

Schork, F.J., 1994. Reactor operation and control. In: McGreavy, C. (Ed.), Polymer Reactor Engineering. Blackie Academic Professional, London, pp. 148–202.

Schork, F.J., Deshpande, P.B., Leffew, K.W., 1993. Control of Polymerization Reactors. Marcel Dekker, Inc., New York.

Schuler, H., Schmidt, Chr.-U., 1992. Calorimetric-state estimators for chemical reactor diagnosis and control: review of methods and applications. Chemical Engineering Science 47 (4), 899–915.

Thomas, I.M., Kiparissides, C., 1984. Computation of near-optimal temperature and initiator policies for a batch polymerization reactor. Canadian Journal of Chemical Engineering 62, 284–291.

Tsoukas, A., Tirrell, M., Stephanopoulos, G., 1982. Multiobjective dynamic optimization of semi-batch copolymerization reactors. Chemical Engineering Science 37 (12), 1785–1795.

Vega, E.L., 1997. Modeling and control of tubular solution polymerization reactors. Computational Chemical Engineering 21, 1049–1054.

Vega, M.P., Lima, E.L., Pinto, J.C., 2001. In-line monitoring of weight average molecular weight in solution polymerization using intrinsic viscosity measurements. Polymer 42 (8), 3909–3914.

Vivaldo-Lima, E., Luna-Barcenas, G., Flores-Tlacuahuac, A., Cruz, M.A., Manero, O., 2004. Modeling of nonlinear polyurethane production in batch reactors using a kinetic-probabilistic approach. Industrial Engineering and Chemical Research 41, 5207–5219.

Waechter, A., 2002. An interior point algorithm for large-scale nonlinear optimization with applications in process engineering. Ph.D. Thesis, Carnegie Mellon University, USA.

Waechter, A., Biegler, L.T., 2004. On the implementation of an interior point filter line search algorithm for large-scale nonlinear programming. Computers and Chemical Engineering, accepted for publication.

Zaldivar, C., Iglesias, G., DelSol, O., Pinto, J.C., 1997. On the preparation of acrylic acid/vinyl acetate copolymer with constant composition—2. Refractive indexes for in-line evaluation of monomer conversion and copolymer composition. Polymer 39 (1), 247–251.

Further Reading

Fontoura, J.M.R., Santos, A.F., Silva, F.M., Lenzi, M.K., Lima, E.L., Pinto, J.C., 2003. Monitoring and control of styrene solution polymerization using NIR spectroscopy. Journal of Applied Polymer Science 90 (5), 1273–1289.

Othman, N.S., Fevotte, G., Peycelon, D., Egraz, J.B., Suau, J.M., 2004. Control of polymer molecular weight using near infrared spectroscopy. A.I.Ch.E. Journal 50 (3), 654–664.

Santos, A.F., Lima, E.L., Pinto, J.C., 2000. Control and design of average particle size in styrene suspension polymerizations using near-infrared spectroscopy. Journal of Applied Polymer Science 77 (2), 453–462.

Vieira, R.A.M., Sayer, C., Lima, E.L., Pinto, J.C., 2002a. Closed-loop composition and molecular weight control of a copolymer latex using near-infrared spectroscopy. Industrial Engineering and Chemical Research 41 (12), 2915–2930.

Vieira, R.A.M., Sayer, C., Lima, E.L., Pinto, J.C., 2002b. In line and in situ monitoring of semi-batch emulsion copolymerizations using near-infrared spectroscopy. Journal of Applied Polymer Science 84 (14), 2670–2682.